

Optical Engineering

OpticalEngineering.SPIEDigitalLibrary.org

Single-mode porous fiber for low-loss polarization maintaining terahertz transmission

Sohel Rana
Md. Saiful Islam
Mohammad Faisal
Krishna Chandra Roy
Raonaqul Islam
Shubi F. Kaijage

SPIE.

Sohel Rana, Md. Saiful Islam, Mohammad Faisal, Krishna Chandra Roy, Raonaqul Islam, Shubi F. Kaijage, "Single-mode porous fiber for low-loss polarization maintaining terahertz transmission," *Opt. Eng.* 55(7), 076114 (2016), doi: 10.1117/1.OE.55.7.076114.

Single-mode porous fiber for low-loss polarization maintaining terahertz transmission

Sohel Rana,^{a,*} Md. Saiful Islam,^b Mohammad Faisal,^c Krishna Chandra Roy,^d Raonaqul Islam,^a and Shubi F. Kaijage^e

^aRajshahi University of Engineering and Technology, Department of Electrical and Electronic Engineering, P.O. Box 6204, Rajshahi, Bangladesh

^bIslamic University of Technology, Department of Electrical and Electronic Engineering, P.O. Box 1704, Gazipur, Bangladesh

^cBangladesh University of Engineering and Technology, Department of Electrical and Electronic Engineering, P.O. Box 1000, Dhaka, Bangladesh

^dBangladesh University of Engineering and Technology, Institute of Information and Communication Technology, P. O. Box 447, Arusha, Bangladesh

^eNelson Mandela African Institution of Science and Technology, Department of Communication Science and Engineering, School of Computational and Communication Science and Engineering, Arusha 23311, Tanzania

Abstract. We report on a polymer-based porous-core photonic crystal fiber for simultaneous high-birefringent and low-loss propagation of narrowband terahertz (THz) electromagnetic waves. The high birefringence is induced by using rotated elliptical air holes inside the porous-core. The fiber is numerically analyzed with an efficient finite-element method. The simulation results exhibit an extremely high birefringence of ~ 0.042 and a very low effective material loss of $\sim 0.07 \text{ cm}^{-1}$ at an operating frequency of 1 THz. Moreover, we have found an optimal rotation angle (θ) = $n30$ deg (n is an odd integer). Other modal features of the fiber, such as confinement loss, power fraction, effective area, bending loss, and dispersion, also have been analyzed. We anticipate that the proposed fiber would be suitable in polarization maintaining THz wave guidance applications. © 2016 Society of Photo-Optical Instrumentation Engineers (SPIE) [DOI: 10.1117/1.OE.55.7.076114]

Keywords: birefringence; polarization; photonic crystal fiber; terahertz.

Paper 160679 received May 2, 2016; accepted for publication Jul. 6, 2016; published online Jul. 25, 2016.

1 Introduction

Recent development in terahertz (THz) technology has made it possible to exploit THz or far infrared rays (10^{11} to 10^{13} Hz) in the fields of biosensing, imaging, spectroscopy, military security,^{1,2} and biomedical engineering.³ One of the most promising applications of the proposed photonic crystal fiber (PCF) concept is associated with noninvasive, minimally invasive and intraoperative medical diagnosis. It could be used for noninvasive early diagnosis of skin cancer, including the basal cell carcinoma,⁴ dysplastic skin nevi, and melanomas⁵ of hardly accessible skin areas; for minimally invasive diagnosis of colon tissue cancers;⁶ or for intraoperative diagnosis of breast tumors.⁷ The devices used for generating and detecting THz waves are readily available,⁸ but it is hard to find an overall efficient waveguide for THz propagation. The reason is that most of the dielectric materials exhibit high absorption loss in the THz regime.⁹ It is well known that dry air works as a transparent medium for THz waves. That is why THz rays are generally transmitted in the free space where proper alignment and maintenance are highly required.

Polarization maintenance (PM) in THz regime also has promising applications in polarization maintaining time-domain spectroscopy.¹⁰ To date, different kinds of waveguides have been proposed for PM THz transmission, which include air core band-gap fibers,¹¹ porous fibers,^{8,12–15} and elliptical dielectric coated metallic hollow fibers.¹⁶ To reduce the fiber propagation loss to some extent, the solid core of the plastic PCF was later replaced with an air core.¹¹ In the meantime, there were reports on squeezed lattice elliptical-hole structures,¹² porous fibers with rectangular slots,^{13,14}

and porous fibers with rotated elliptical air holes.¹⁵ The works described in Refs. 13 and 14 showed high birefringence of ~ 0.026 and the one in Ref. 15 showed an ultrahigh birefringence of ~ 0.045 . Very recently, Islam et al.⁸ proposed a porous fiber with rectangular slots that exhibits a high birefringence of ~ 0.075 and effective material loss (EML) of 0.07 cm^{-1} . Tang et al.¹⁶ presented a metallic hollow fiber with dielectric coating that exhibits a high-modal birefringence ($\sim 1.36 \times 10^{-2}$). It also allows propagating a majority of the mode power through an elliptical air core resulting in a very low effective absorption loss ($\sim 0.003 \text{ cm}^{-1}$). Raonaq et al.¹⁷ proposed a porous fiber based on dual asymmetry that shows a high birefringence of 0.045 and EML of 0.08 cm^{-1} . Recently, Hasanuzzaman et al.¹⁸ reported a novel design based on dual unit air holes in the core instead of one hole that exhibits a high birefringence of 0.033 and EML of $\sim 0.43 \text{ dB/cm}$ (or equivalent to 0.09 cm^{-1}). Note that all the previous reports analyzed one or two optical properties simultaneously such as low birefringence, high absorption loss, and fabrication difficulties. Reviewing the literatures so far, it is realized that two distinct but effective methods are used to obtain high birefringence in the THz regime; one is to break the symmetry of the fiber cladding,¹⁹ and the other is to achieve asymmetric characteristics in the fiber core.^{20,21}

In this paper, we present a porous-core PCF, which has elliptical air holes in the core and circular air holes arranged in a hexagonal lattice in the cladding. Rotation of the elliptical air holes at an optimum angle successfully breaks the symmetry of the fiber core and hence induces a high birefringence of ~ 0.042 . Also, most of the power is transmitted through air media exhibiting a low effective material loss

*Address all correspondence to: Sohel Rana, E-mail: dsmsrana@gmail.com

(EML) of $\sim 0.07 \text{ cm}^{-1}$. In addition, it also unveils ultra-low confinement loss in the order of 10^{-3} cm^{-1} and low bending loss in the order of 10^{-1} cm^{-1} with its optimal design parameters. Although porous fiber with elliptical air holes in the core and air-cladding,¹⁵ porous fiber based on dual asymmetry¹⁷ and dual unit-based porous fiber¹⁸ have already been studied, to our knowledge, a porous fiber features hexagonal arrays of air holes in the cladding and rotated elliptical air holes in the core has never been investigated before in the THz regime for the modal properties of a fiber such as EML, birefringence, effective area, confinement loss, bending loss, and dispersion simultaneously.^{8,11-18}

2 Design Principle

The cross section of the proposed THz fiber is shown in Fig. 1. For simplicity, a hexagonal structure is considered for both the core and the cladding regions of the proposed design. The air holes are arranged in triangular lattices where the symbols Λ and Λ_c represent the distance between two adjacent air holes in cladding and core regions, respectively. The diameters of the major and minor axes of the elliptical air holes in the core are denoted by M and N . We adjust the core diameter [$D_{\text{core}} = 2(\Lambda - d/2)$] in between 150 and 250 μm , whereas the normalized ratio (d/Λ) is kept constant at 0.95 for a good confinement factor. The diameter of the air holes of the cladding is denoted by d . In our design, we use $M = 14.4 \mu\text{m}$, $N = 5.6 \mu\text{m}$, $D_{\text{core}} = 200 \mu\text{m}$, $d = 180 \mu\text{m}$, and whole radius of the fiber is 1067 μm . These values of parameters are chosen for better results such as low EML, confinement loss, bending loss, high birefringence, and power fraction. The background material chosen for this fiber is cyclic-olefin copolymer with a trade name of TOPAS. It has some decisive advantages over other polymer materials (PMMA, Teflon, HDPE, etc.) such as low bulk material loss of 0.2 cm^{-1} at $f = 1 \text{ THz}$,²² a constant refractive index of $n = 1.5258$ between 0.1 and 2 THz frequency range, humidity insensitivity,²³ and chemical inertness with special biosensing properties.²⁴

3 Results and Discussions

To compute the modal properties of the proposed fiber, we utilized the finite-element method-based commercially available software COMSOL. An artificial absorbing layer, known as the perfectly matched layer (PML), is applied outside the structure to limit the computational domain and minimize nonphysical back scattering. In our design,

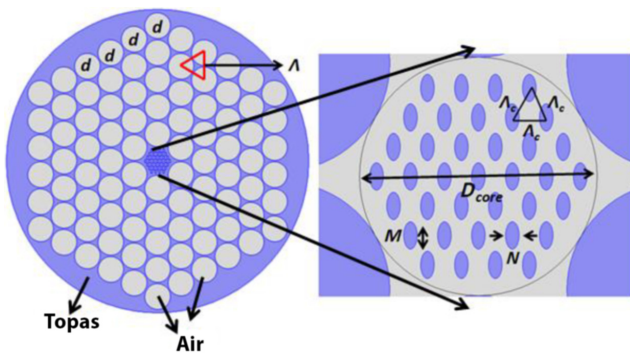


Fig. 1 Cross section of proposed fiber and the extended view of its core at rotation angle (θ) = 0 deg.

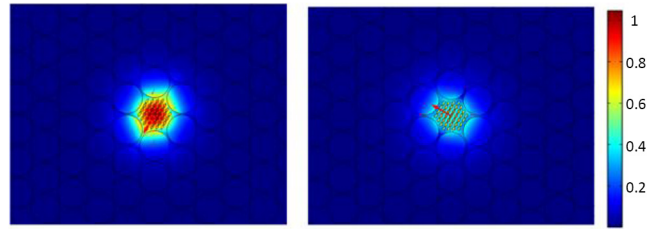


Fig. 2 Electric field distribution of the normalized power flow for x and y polarization modes at $D_{\text{core}} = 200 \mu\text{m}$, $f = 1 \text{ THz}$ and rotation angle (θ) = 30 deg.

the thickness of the PML region is 9% of the total radius of the fiber. Figure 2 shows the power flow distribution of the proposed fiber for the two orthogonal polarization modes, which strongly illustrates that mode power is well confined within the fiber core. Throughout the analytical process, the parameters are chosen such that the single-mode condition always is fulfilled.

First, the single-mode condition is verified with V -parameter expressed as¹⁵

$$V = \frac{2\pi r f}{c} \sqrt{n_{\text{co}}^2 - n_{\text{cl}}^2} \leq 2.405, \tag{1}$$

where r is the radius of the core, c is the velocity of electromagnetic waves in vacuum, n_{co} and n_{cl} are the refractive indices of the core and the cladding, respectively. We have assumed n_{cl} as a unity¹⁵ because the cladding is densely populated with air holes. On the other hand, n_{co} is regarded as n_{eff} because of the porous core. Eq. (1) means V -parameter of the proposed fiber should be kept lower or equal to 2.405 in order to achieve the single-mode property. We have shown the V -parameter with respect to frequency in Fig. 3, where it is noticed that for both the orthogonal polarization modes, the fiber maintains the single-mode property when $f \leq 1.45 \text{ THz}$. Hence, our study is based on the frequency range of 0.7 to 1.45 THz.

Now, the birefringence of the PCF is quantified by¹⁵

$$B = |n_x - n_y|, \tag{2}$$

where B indicates birefringence, n_x and n_y are the refractive indices of x and y polarization modes, respectively. Figure 4

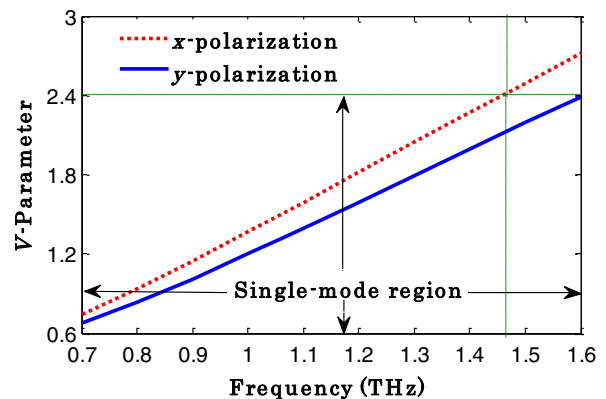


Fig. 3 V -parameter as a function of frequency at $D_{\text{core}} = 200 \mu\text{m}$ and rotation angle (θ) = 30 deg. The dashed lines show the single-mode boundary condition.

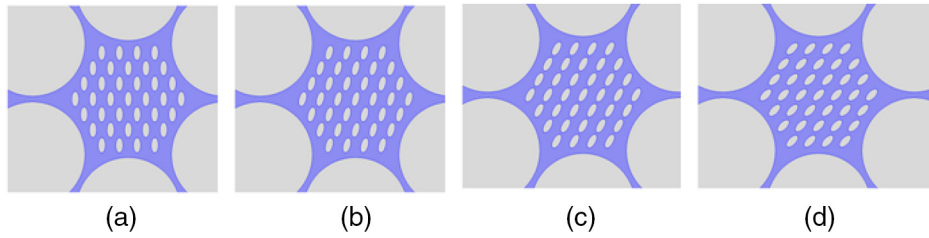


Fig. 4 Elliptical air holes in the core at different rotational angles: (a) 0 deg, (b) 15 deg, (c) 30 deg, and (d) 45 deg.

depicts the cross section of the core at various rotation angles. The birefringence with respect to rotation angle is shown in Fig. 5, where it is observed that maximum birefringence can be obtained at $\theta(\text{deg}) = n30$ deg (n is an odd integer). Likewise, minimum birefringence is obtained when n is an even integer. The physical reason is that when the rotation angle is an odd multiple of 30 deg, the elliptical air holes arrange themselves in such a way that the major axes of multiple air holes are synchronized [refer Fig. 4(c)]. As a result, the symmetry of the porous-core is broken along a fixed direction to induce maximum birefringence for this arrangement. On the other hand, when the rotation angle is an even multiple of 30 deg, the major axes of every air hole are arranged at different angles to induce the minimum birefringence [see Fig. 4(a)]. We found that the proposed fiber shows a birefringence of ~ 0.042 at $\theta(\text{deg}) = n30$ (n is an odd integer), exhibited in Fig. 5, which is very much comparable to the previously reported works.^{8,11–18} Note that birefringence can be further enhanced by increasing the ratio of major axis length (M) to minor axis length (N) of elliptical air holes. But it leads to high material absorption loss. In contrast, effective refractive index for both polarizations also changes while ratio (M/N) is varied.

Figure 6 shows the birefringence as a function of frequency, where it is observed that the birefringence value increases with frequency. This is due to the fact that at a higher frequency, more power is propagated through the elliptical air holes. It can also be observed from Fig. 6 that $\theta(\text{deg}) = n30$ (n is an odd integer) (for this case 30 deg) features high birefringence value as compared to the rest (0, 15, and 45 deg).

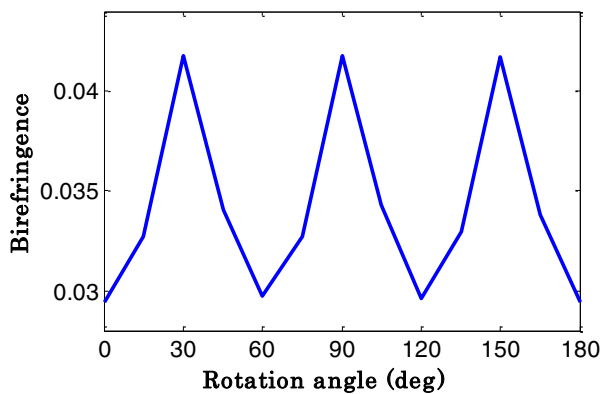


Fig. 5 Birefringence versus rotation angles at $D_{\text{core}} = 200 \mu\text{m}$ and $f = 1 \text{ THz}$.

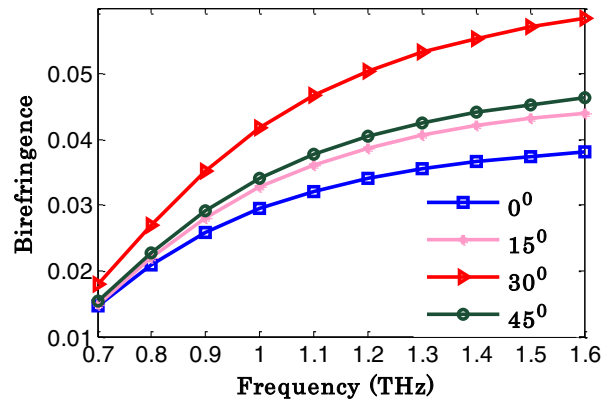


Fig. 6 Birefringence versus frequency at different rotation angles for $D_{\text{core}} = 200 \mu\text{m}$.

Another important modal property to be analyzed for THz fibers is the EML or the effective absorption loss (α_{eff}), which can be calculated using²³

$$\alpha_{\text{eff}} = \sqrt{\frac{\epsilon_0}{\mu_0}} \left(\frac{\int_{\text{mat}} n_{\text{mat}} |E|^2 \alpha_{\text{mat}} dA}{|\int_{\text{all}} S_z dA|} \right), \quad (3)$$

where ϵ_0 and μ_0 are the permittivity and permeability of the vacuum, n_{mat} is the refractive index of the material used, E is the modal electric field, α_{mat} is the bulk material absorption loss, and S_z is the z -component of the Poynting vector, $S_z = (1/2)(\vec{E} \times \vec{H}^*) \cdot \hat{z}$. In our proposed fiber, we examined the intensity EML of the THz wave. EML as a function of frequency is shown in Fig. 7, where it is observed that the

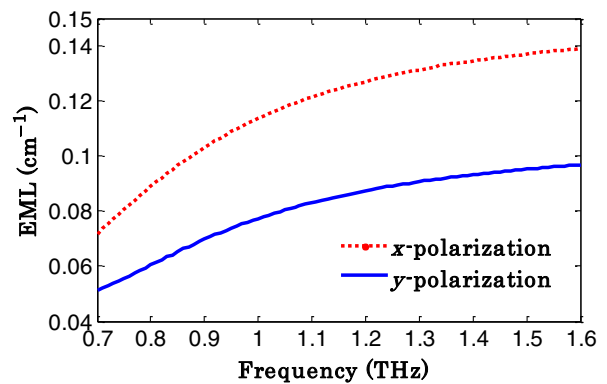


Fig. 7 EML as a function of frequency at $D_{\text{core}} = 200 \mu\text{m}$ and rotation angle (θ) = 30 deg.

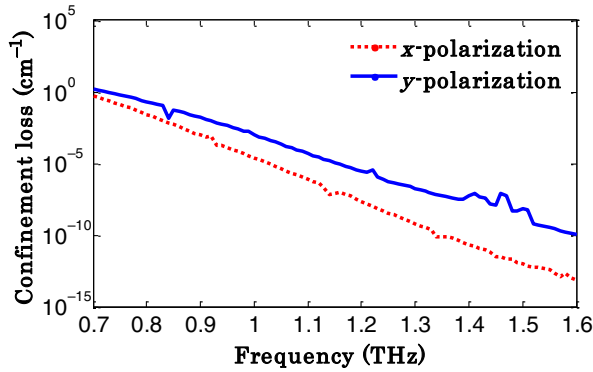


Fig. 8 Confinement loss as a function of frequency at $D_{\text{core}} = 200 \mu\text{m}$ and rotation angle $(\theta) = 30 \text{ deg}$.

loss is increased with the frequency for both polarizations, respectively, because EML is proportional to electromagnetic wave frequency and the imaginary part of the effective refractive index. Note that $f = 1 \text{ THz}$ and $D_{\text{core}} = 200 \mu\text{m}$, the EML is $\sim 0.07 \text{ cm}^{-1}$ for y -polarization mode and $\sim 0.1137 \text{ cm}^{-1}$ for x -polarization mode, which is comparable to the previously reported highly birefringent fibers.^{8,11–18}

The boundary limitation of the periodic cladding of a fiber introduces the confinement loss. It is obtained from the imaginary part of the complex refractive index (n_{eff}) given by²⁵

$$\alpha_{\text{CL}} = 8.686k_0 \text{Im}(n_{\text{eff}}), \quad (4)$$

where $k_0 = 2\pi/\lambda$ and $\text{Im}(n_{\text{eff}})$ is the imaginary part of the refractive index of the guided mode. The simulated confinement loss is shown in Fig. 8, which shows the decrement of confinement loss with increasing frequency. It is due to the fact that some of the mode power penetrates into the cladding region when frequency is increased. Figure 8 also shows few peaks for both polarization and it is maybe for changes of effective refractive index with frequency variation. It is observed that the confinement loss is very low and negligible compared to the EML for both the polarization modes at the optimal parameters at $f > 0.85 \text{ THz}$.

At this point, we discuss the fraction of mode power propagated through different regions of the fiber. The mode power fraction can be estimated using¹⁵

$$\eta' = \frac{\int_X S_z dA}{\int_{\text{all}} S_z dA}, \quad (5)$$

where X represents the integral region of interest. Our main concern is to transmit most of the mode power through the elliptical air holes in order to simultaneously achieve high-birefringence and low EML values. Figure 9 shows the power fraction in different regions with respect to frequency. One can deduce from Fig. 9 that 21% and 26% of the total transmitted power goes through the elliptical core air holes for x and y polarization modes, respectively, at $f = 1 \text{ THz}$. Also, it can be realized that there is a decrement of transmitted power in the cladding area as frequency increases, the outcome of which agrees with the increased transmitted power in the air holes of the core.

We also characterize the modal effective area (A_{eff}) of the proposed fiber. The effective area of the fundamental mode can be quantified by²⁶

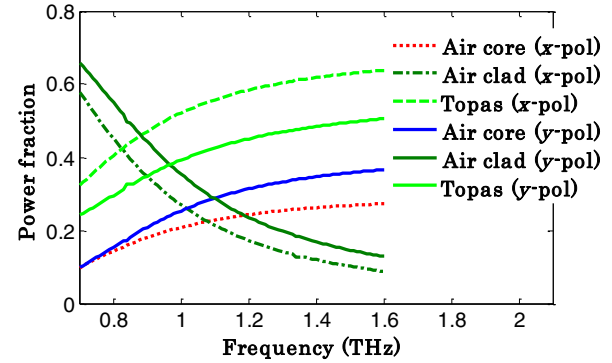


Fig. 9 Mode power fraction as a function of frequency in different regions of the proposed fiber at $D_{\text{core}} = 200 \mu\text{m}$ and rotation angle $(\theta) = 30 \text{ deg}$.

$$A_{\text{eff}} = \frac{\left[\int I(r) r dr \right]^2}{\left[\int I^2(r) dr \right]^2}, \quad (6)$$

where $I(r) = |E_t|^2$ is the transverse electric field intensity distribution in the fiber cross section. Figure 10 shows the A_{eff} as a function of frequency. At this point, we would like to point out an interesting observation that the modal effective area A_{eff} changes its behavior at $f = 0.9 \text{ THz}$. It is because of more light spread into y -polarized wave for $f < 0.9 \text{ THz}$ and converse for $f > 0.9 \text{ THz}$. It is also observed that at operating parameters the calculated A_{eff} is very much comparable to those in Refs. 25 and 26.

To further investigate the impact of design parameters, the loss induced due to macrobending is calculated by replacing the bent fiber with an equivalent straight fiber. A conformal transformation method²⁷ is used to calculate the effective mode index of the equivalent fiber (n_{eq}), which is used to calculate the leakage loss. n_{eq} is given as²⁷

$$n_{\text{eq}}(x, y) = n(x, y) \exp(1 + x/R), \quad (7)$$

where $n(x, y)$ is the original refractive index of the fiber, R is the bending radius, and x is the distance from the center of the fiber along x -axis. After the equivalent index is calculated, bending loss can be found by using the same formula described in Eq. (4). The bending loss characteristic of the

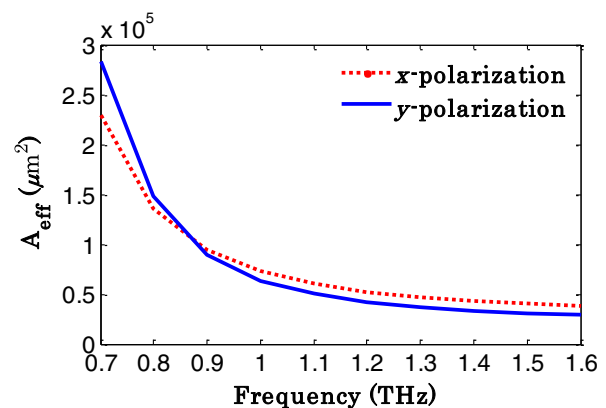


Fig. 10 Effective mode area as a function of frequency at $D_{\text{core}} = 200 \mu\text{m}$ and rotation angle $(\theta) = 30 \text{ deg}$.

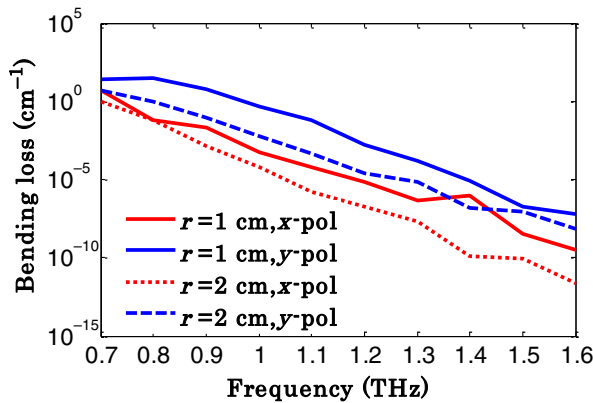


Fig. 11 Bending loss as a function of frequency at different bending radii and $D_{\text{core}} = 200 \mu\text{m}$ and rotation angle $(\theta) = 30$ deg.

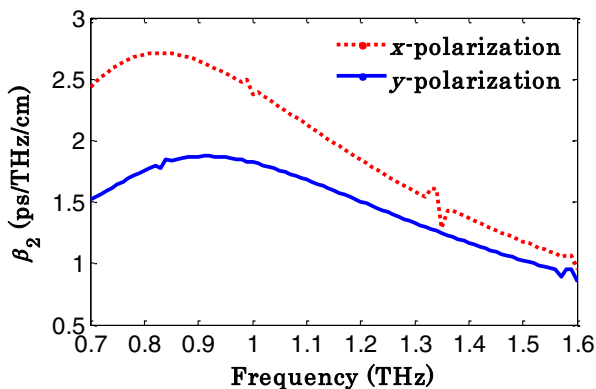


Fig. 12 Dispersion parameter versus frequency at $D_{\text{core}} = 200 \mu\text{m}$ and rotation angle $(\theta) = 30$ deg.

proposed fiber is shown in Fig. 11, where it is observed that the loss reduced with increasing bend radius and frequency. It is also observed that the x -polarization mode shows a lower loss than the y -polarization mode.

Next, we calculated the dispersion of the proposed fiber. Since the refractive index of TOPAS is constant between the $f = 0.1$ and 2 THz,²³ our proposed fiber shows only the waveguide dispersion. The dispersion parameter is calculated by²⁸

$$\beta_2 = \frac{2}{c} \frac{dn_{\text{eff}}}{d\omega} + \frac{\omega}{c} \frac{d^2 n_{\text{eff}}}{d\omega^2}, \quad (8)$$

where angular center frequency $\omega = 2\pi f$ and c is the velocity of electromagnetic waves. Figure 12 displays the dispersion characteristics where it is observed that a positive low and flat dispersion (1 to 2.7 ps/THz/cm) is obtained within the operating frequency range at optimal parameters. As frequency increases, the refractive index of the fiber for both polarization changes and some mode power penetrates into the cladding. As a result, some fluctuations and peaks are observed in Fig. 12.

Also, it is important to note something about the fabrication possibility of the proposed fiber. Elliptical air holes as can be seen from Fig. 1, during the fabrication process, can be vulnerable and hence collapse to become circular. Fortunately, this can be solved by using a new multistep

process of forming preforms²⁹ that can overcome these difficulties. Even though the method used is to demonstrate circular air hole shapes, it is still our expectation that due to technological advances the method would be extended to fabricate elliptical air holes in the near future. Recently, the EFG/Stepanov technique³⁰ has attracted the attention of researchers for manufacturing THz waveguide. It is due to the fact that the EFG/Stepanov technique based on sapphire-shaped crystal is suitable for manufacturing the THz waveguides characterized with low loss and dispersion.

4 Conclusion

We have demonstrated a highly birefringent porous fiber for polarization maintaining propagation of THz waves. The key features of the proposed fiber are its simultaneously exhibited properties; high-birefringence, low EML, low confinement loss, low bending loss, and low dispersion generated with the hexagonal lattice cladding. The holey cladding also protects the radiation from atmospheric infiltration. We believe, with the assistance of advanced technology, the proposed fiber would be engineered and used in polarization maintaining THz appliances.

References

1. M. M. Awad and R. A. Cheville "Transmission terahertz waveguide-based imaging below the diffraction limit," *Appl. Phys. Lett.* **86**(22), 221107 (2005).
2. D. J. Cook, B. K. Decker, and M. G. Allen, "Quantitative THz spectroscopy of explosive materials," in *Proc. of OSA Conf. on Optical Terahertz Science and Technology*, pp. 1–4 (2005).
3. R. M. Woodward et al., "Terahertz pulsed imaging of skin cancer in the time and frequency domain," *J. Biol. Phys.* **29**(2–3), 257–261 (2003).
4. V. P. Wallace et al., "Terahertz pulsed imaging of basal cell carcinoma ex vivo and in vivo," *Br. J. Dermatol.* **151**(2), 424–432 (2004).
5. K. I. Zaytsev et al., "In vivo terahertz spectroscopy of pigimentary skin nevi: pilot study of non-invasive early diagnosis of dysplasia," *Appl. Phys. Lett.* **106**(5), 053702 (2015).
6. C. B. Reid et al., "Terahertz pulsed imaging of freshly excised human colonic tissues," *Phys. Med. Biol.* **56**(14), 4333–4353 (2011).
7. P. C. Ashworth et al., "Terahertz pulsed spectroscopy of freshly excised human breast cancer," *Opt. Express* **17**(15), 12444–12454 (2009).
8. R. Islam et al., "Extremely high-birefringent asymmetric slotted-core photonic crystal fiber in THz regime," *IEEE Photonics Technol. Lett.* **27**(21), 2222–2225 (2015).
9. H. Bao et al., "Dielectric tube waveguides with absorptive cladding for broadband, low-dispersion and low loss THz guiding," *Sci. Rep.* **5**, 7620 (2015).
10. M. B. Byrne et al., "Simultaneous measurement of orthogonal components of polarization in a free-space propagating terahertz signal using electro-optic detection," *Appl. Phys. Lett.* **98**(15), 151104 (2011).
11. G.-B. Ren et al., "Polarization maintaining air-core bandgap fibers for terahertz wave guiding," *IEEE J. Quantum Electron.* **45**(5), 506–513 (2009).
12. H. Chen, D. Chen, and Z. Hong, "Squeezed lattice elliptical hole terahertz fiber with high birefringence," *Appl. Opt.* **48**(20), 3943–3947 (2009).
13. S. Atakaramians et al., "Low loss, low dispersion and highly birefringent terahertz porous fibers," *Opt. Commun.* **282**(1), 36–38 (2009).
14. S. Atakaramians et al., "THz porous fibers: design, fabrication and experimental characterization," *Opt. Express* **17**(16), 14053–14062 (2009).
15. N. Chen, J. Liang, and L. Ren, "High-birefringence, low-loss porous fiber for single-mode terahertz-wave guidance," *Appl. Opt.* **52**(21), 5297–5302 (2013).
16. X.-L. Tang, B.-S. Sun, and Y.-W. Shi, "Design and optimization of low loss high birefringence hollow fiber at terahertz frequency," *Opt. Express* **19**(25), 24967–24679 (2011).
17. R. Islam et al., "Novel porous fiber based on dual-asymmetry for low-loss polarization maintaining THz wave guidance," *Opt. Lett.* **41**(3), 440–443 (2015).
18. G. K. M. Hasanuzzaman, S. Rana, and M. S. Habib, "A novel low loss, highly birefringent photonic crystal fiber in THz regime," *IEEE Photonics Technol. Lett.* **28**(8), 899–902 (2015).
19. Y. Yue et al., "Highly birefringent elliptical-hole photonic crystal fiber with squeezed hexagonal lattice," *Opt. Lett.* **32**(5), 469–471 (2007).

20. S. E. Kim et al., "Elliptical defected core photonic crystal fiber with high birefringence and negative flattened dispersion," *Opt. Express* **20**(2), 1385–1391 (2012).
21. D. R. Chen and L. F. Shen, "Highly birefringent elliptical-hole photonic crystal fibers with double defects," *J. Lightwave Technol.* **25**(9), 2700–2705 (2007).
22. K. Nielsen et al., "Bendable, low-loss TOPAS fibers for the terahertz frequency range," *Opt. Express* **17**(10), 8592–8601 (2009).
23. G. Emiliyanov et al., "Localized biosensing with TOPAS microstructured polymer optical fiber," *Opt. Lett.* **32**(5), 460–462 (2007).
24. G. Emiliyanov et al., "Selective serial multi-antibody biosensing with TOPAS microstructured polymer optical fibers," *Sensors*, **13**, 3242–3251 (2013).
25. S. F. Kaijage, Z. Ouyang, and X. Jin, "Porous-core photonic crystal fiber for low loss terahertz wave guiding," *IEEE Photonics Technol. Lett.* **25**(15), 1454–1457 (2013).
26. J. J. Bai et al., "A porous terahertz fiber with randomly distributed air holes," *Appl. Phys. B* **103**(2), 381–386 (2011).
27. M. Heiblum and J. Harris, "Analysis of curved optical waveguides by conformal transformation," *IEEE J. Quantum Electron.* **11**(2), 75–83 (1975).
28. J. Liang et al., "Broadband, low-loss, dispersion flattened porous-core photonic bandgap fiber for terahertz (THz)-wave propagation," *Opt. Commun.* **295**, 257–261 (2013).
29. P. Falkenstein, C. D. Merritt, and B. L. Justus, "Fused performs for the fabrication of photonic crystal fibers," *Opt. Lett.* **29**, 1858–1860 (2004).
30. K. I. Zaytsev et al., "Terahertz photonic crystal waveguides based on sapphire shaped crystals," *IEEE Trans. Terahertz Sci. Technol. PP*(99), 1–7 (2016).

Sohel Rana received his BSc degree in electrical and electronic engineering from Rajshahi University of Engineering and Technology (RUET), Rajshahi, Bangladesh, in December 2014. Since August 2015, he has been working as a lecturer in the Department of Electrical and Electronic Engineering, Bangladesh University. His research interests are in terahertz wave guiding, optics, and photonics.

Md. Saiful Islam received his BSc degree in electronics and telecommunication engineering from Rajshahi University of Engineering and Technology and is now pursuing an MSc degree in electrical and electronic engineering from Islamic University of Technology, Gazipur,

Bangladesh. His area of interest includes fiber optics and THz signal transmission. He is currently researching the design of optical fibers for long-distance low-loss terahertz wave propagation.

Mohammad Faisal received his BSc (Hons.) and MSc degrees in electrical and electronic engineering (EEE) in 2000 and 2003, respectively, from Bangladesh University of Engineering and Technology (BUET), Dhaka, Bangladesh, and the PhD in electrical, electronic and information engineering from Osaka University, Suita, Japan, in March 2010. He has been with the Department of Electrical and Electronic Engineering, BUET, where he is currently an Associate Professor. His research interests include optical communication and photonics.

Krishna Chandra Roy was born in Dinajpur, Bangladesh, in 1992. He received his BSc degree in electronics and communication engineering from Khulna University of Engineering and Technology, Khulna, Bangladesh, in 2014, and is pursuing the MSc degree in information and communication technology from Bangladesh University of Engineering and Technology. He is currently a Lecturer in the Department of Electrical and Electronic Engineering, Bangladesh University. His current research interests include biomedical imaging, biomedical signal processing, and optical imaging.

Raonaqul Islam received his BSc degree in electrical and electronic engineering from Rajshahi University of Engineering and Technology (RUET), Rajshahi, Bangladesh, in December 2014. His area of interest includes fiber optics and electronics. He is currently researching the design of optical fibers for low-loss terahertz wave propagation.

Shubi F. Kaijage received his Doctor of Engineering (electronics and information engineering) and his Master of Engineering (electrical and electronics engineering) degrees from the University of the Ryukyus, Japan, in March 2011 and March 2008, respectively. Since February 2014, he has been working as a lecturer and head at the School of Computational and Communication Science and Engineering, Nelson Mandela African Institution of Science and Technology, Arusha, Tanzania. His research interests are in photonics, optoelectronics, and terahertz wave technology.